The Study of Multiple Electron Transfer Reactions by Cyclic Voltammetry

Adrian W. Bott, Ph.D.
Bioanalytical Systems
West Lafayette, IN
47906-1382

Phone: 765-463-4527
FAX: 765-497-1102
E-Mail:
awb@bioanalytical.com

The factors that give rise to two-electron transfer processes are discussed and are illustrated by examining the redox behavior of a range of compounds.

Although electron transfer processes involving two electrons are discussed in the literature as "two-electron" processes, it is generally accepted that such processes involve two separate one-electron transfer processes. Analysis of such reactions (e.g., by digital simulation) must therefore be based on the analysis of these one-electron processes. In this article, a number of examples will be used to illustrate some of the characteristic features of cyclic voltammograms of systems that undergo "two-electron" electron transfer processes.

The systems considered in this article are divided into two categories: those with two discrete (localized) redox centers, and those in which the change in charge is delocalized over the entire molecule. However, it should be noted that these descriptions can be considered as the limiting examples of a continuum of structures.

a) Two Localized Redox Centers

Molecules containing two localized redox centers have been widely studied, due to their ability to catalyze reactions that require multiple electron transfers (e.g., the reduction of oxygen). The cyclic voltammograms of such molecules are determined by the separation of the redox potentials of the different centers. If the redox potential of the second electron transfer process (for a net two-electron reduction) is no more than 100 mV more negative than that of the first electron transfer process, then the two processes cannot be resolved; that is, there is only one wave in the cyclic voltammogram. However, the shape of this wave (the peak separation, ΔE_p, and the peak width, E_p-$E_{p/2}$) is determined by the difference in the redox potentials (note that it is also affected by the electron transfer kinetics and the stability of the reactant and product molecules). A plot of ΔE_p vs. $E_1^{o'}$ - $E_2^{o'}$ for a molecule undergoing two one-electron reductions is shown in ***F1*** (1) (these data assume reversibility; that is, rapid electron transfer kinetics and stable reactant and product molecules). It can be seen from this curve that the limiting value of ΔE_p is about 30 mV (2); however, the redox potential of the second reduction must be significantly more positive than that of the first process (i.e., the second process requires less energy than the first) before this limit is reached (if the two redox potentials are the same, then ΔE_p is 42 mV). Molecules in which the second electron transfer process requires less energy than the first process are discussed in the second section of this article.

It is often convenient to discuss the separation of the peak potentials for systems with two redox centers in terms of the comproportionation equilibrium constant of the intermediate (i.e., the product of the first electron transfer reaction). This is given by the equation

$$K_c = exp\left[\frac{(E_1^{o'} - E_2^{o'})\ F}{RT}\right]$$

The separation of the redox potentials $\Delta E^{o'}$ (and hence the magnitude of K_c) is determined by the degree of interaction between the redox centers. It has been shown (3) that $\Delta E^{o'}$ = 35.6 mV when there is no interaction. This translates to a ΔE_p value of 59 mV (using the above plot); that is, the peak parameters are the same as those of a reversible one-electron transfer re-

F1

Plot of peak separation as a function of $E_1^{o'}$ - $E_2^{o'}$ for systems undergoing two one-electron reductions.

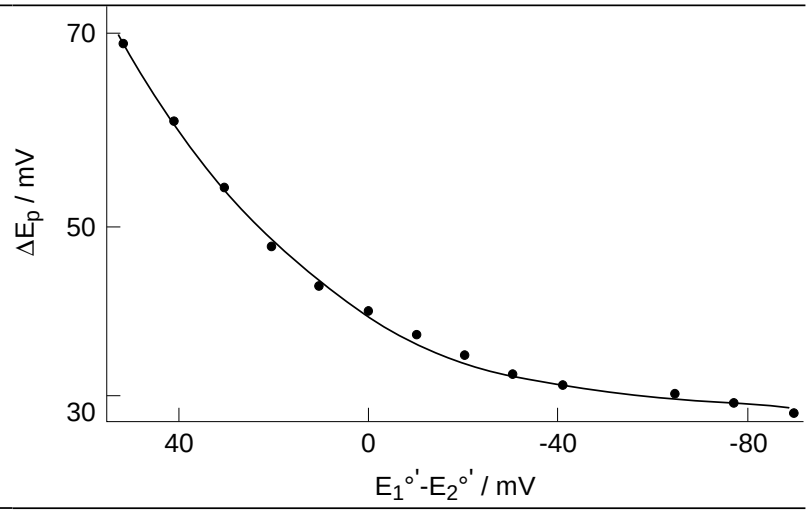

F2

Molecular structures of (a) M_4(PFT) and (b) M_4(OXA) (M = Mo or W; PFT - perfluoroterephthalate; OXA = oxalate).

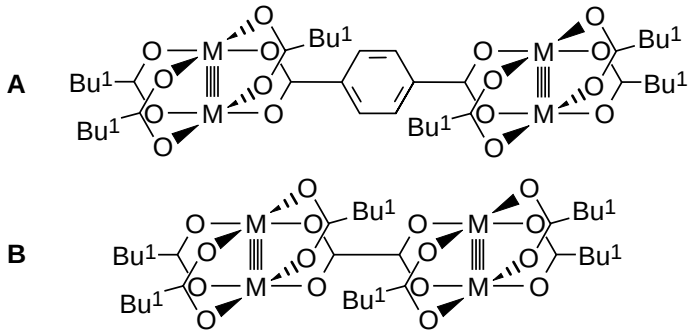

F3

Observed (solid line) and simulated (dashed line) cyclic voltammogram of $Os_6(CO)_{18}$ (figure adapted from reference 6).

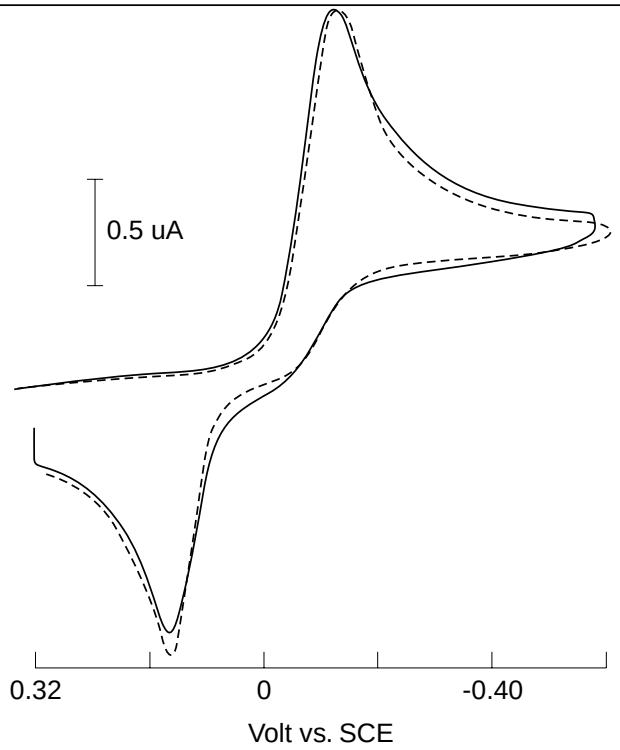

action, the only difference being an increase in the peak current. Systems showing minimal or no interaction (values of K_c less than 100) are classified as Class I according to the Robin-Day scheme (4). The electron transfer reactions of Class I molecules can be considered in terms of the oxidation states of the individual redox centers; that is, the reduction of a bimetallic molecules can be represented as

$$M(III)M(III) + 2e^- = [M(II)M(II)]2^-$$

As the degree of interaction increases, ΔE^o and K_c also increase. Values of K_c greater than 10^6 indicate extensive delocalization of charge between the redox centers, and such systems are classifed as Class III. The extensive delocalization means that the redox properties cannot be considered in terms of the oxidation states of the individual redox centers, and a molecular orbital description is required; that is,

$$M_2 + e^- = M_2^-$$
$$M_2^- + e^- = M_2^{2-}$$

Class II systems show an intermediate degree of delocalization ($100 < K_c < 10^6$). Although there is some delocalization between the metal centers, the redox properties can still be considered in terms of the oxidation states of the individual redox centers; that is,

$$M(III)M(III) + e^- = [M(III)M(II)]^-$$
$$[M(III)M(II)]^- + e^- = [M(II)M(II)]^{2-}$$

Since the two redox potentials are well separated, the product of the first electron transfer reaction (generally referred to as the mixed-valence intermediate) can sometimes be isolated. Such species are characterized by an absorption in the visible spectrum due to charge transfer between the two redox sites (termed the intervalence band).

The variation of the cyclic voltammetric behavior with the degree of interaction between the two redox centers has been illustrated by a series of tetranuclear molybdenum and tungsten molecules (5). These molecules consist of two quadruply-bonded M_2 units (M_2 = Mo_2 or W_2) linked by an organic ligand L (***F2***). The degree of interaction between the two units depends on a) the coupling ligand and b) the met-

F4

Interconversion of $Os_6(CO)_{18}$ and $[Os_6(CO)_{18}]^{2-}$ (each circle represents an $Os(CO)_3$ group).

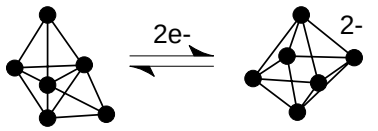

F5

Cyclic voltammograms of 1 mM $[(\eta^6\text{-}C_6Me_6)_2Ru]^{2+}$ in acetonitrile at scan rates of (a) 0.1 V s^{-1} and (b) 50 V s^{-1} (figure adapted from reference 7).

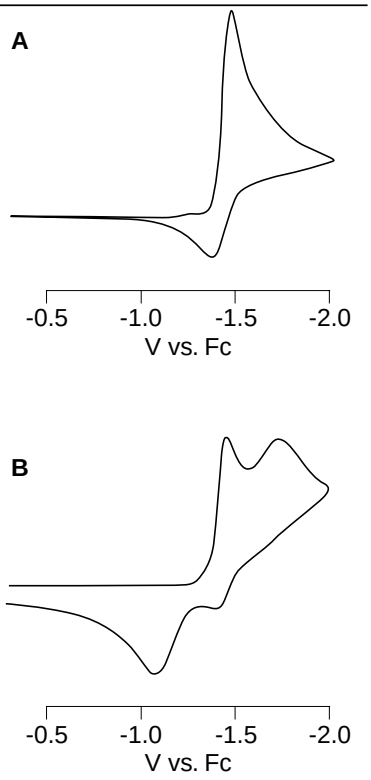

F6

Interconversion of $[(\eta^6,\eta^6C_6Me_6)_2Ru]^{2+}$, $[(\eta^6,\eta^6C_6Me_6)_2Ru]^{+}$, and $[(\eta^6,\eta^4C_6Me_6)_2Ru]$.

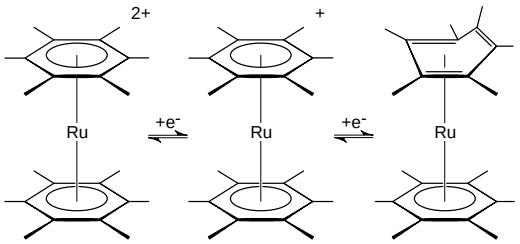

al. When L = perfluoroterephthalate (***F2A***) and M = Mo, there is little interaction between the two Mo_2 centers, and only one oxidation is evident (K_c = 13). However, when L = oxalate (***F2B***), there is some delocalization of charge between the M_2 centers, and two oxidations can be seen ($K_c = 5.4 \times 10^4$) (the greater delocalization was attributed to shorter bridging group). Substituting Mo with W also increases the extent of the delocalization; for L = perfluoroterephthalate, $K_c = 6.6 \times 10^4$, and for L = oxalate, $K_c = 1.3 \times 10^{12}$.

b) One Redox Center

In this section, we will consider molecules in which the electrons are added to or removed from a molecular orbital delocalized over the entire molecule, rather than localized at an electronically isolated center. This description is similar to that used to describe Class III molecules above. However, since the two electrons added to Class III molecules are added to the same molecular orbital, the energy required for the addition (or removal) of the second electron must be greater than that required for the addition (or removal) of the first electron. Therefore, Class III molecules display two separate one-electron processes. For delocalized molecules to undergo a "two-electron" reduction (i.e., only one wave can be seen), the second reduction must require less energy than the first. The greater ease of the second reduction is typically a result of either a change in the molecular structure subsequent to or concomitant with the first reduction, or destabilization of the intermediate by changes in solvation. Characterization of these "two-electron" processes therefore requires investigation of the constitutent one-electron reactions and the coupled chemical reactions.

$Os_6(CO)_{18}$ undergoes a two-electron reduction to $[Os_6(CO)_{18}]^{2-}$ (***F3***) (6). This reduction is accompanied by a change in the metal geometry from a bicapped octahedron to an octahedron (***F4***). Although a good match between the experimental and simulated data could be obtained by simulating a two-electron process, the kinetic parameters obtained are related to *both* electron transfer steps, and provide little information about the *individual* electron transfer reactions. Analysis of the cyclic voltammograms in terms of the two one-electron processes showed that the change in the metal geometry occurred during the first reduction. Since an octahedral structure has one more bonding molecular orbital than a bicapped tetrahedron, this change in structure transforms the monoanion from an electron-rich intermediate that would be more difficult to reduce than the neutral molecule to an electron-deficient intermediate that is more easily reduced than the starting molecule. Therefore, the potential required for the second reduction is less negative than that required for the first reduction.

The effect of solvent on redox potentials is illustrated by the cyclic voltammograms of $[(\eta^6\text{-}C_6Me_6)_2Ru]^{2+}$ at low scan rate (7). When methylene chloride is used as the solvent, two one-electron reductions can be resolved. However, when acetonitrile is used, a single two-electron process is observed. This was attributed to a negative shift of the redox potential for the first reduction due to the preferential solvation of more positively charged species by acetonitrile (i.e., the dication is stabilized by solvation). The separation of the two reduction processes by varying the solvent was referred to as *thermodynamic* discrimination. Upon increasing the scan rate from 0.1 V s^{-1} to 10 V s^{-1} and above (***F5***), the single two-electron process recorded when using acetonitrile as the solvent was split into two one-electron processes. This *kinetic* discrimination was possible due to the large increase in ΔE_p for the second reduction relative to that of the first reduction (the electron transfer rate constants were found to be 2.0 and 4.5×10^{-4} cm s^{-1} for the first and second reductions respectively) and the small difference in the redox potentials (0.03 V). The slow rate of electron transfer for the second step was consistent with the change in the coordination mode of one of the ligands (from six-coordinate to four-coordinate) that occurred during this step (***F6***). The driving force

F7

Molecular structure of [Rh(μ-t-Bu$_2$P)(CO)$_2$]$_2$.

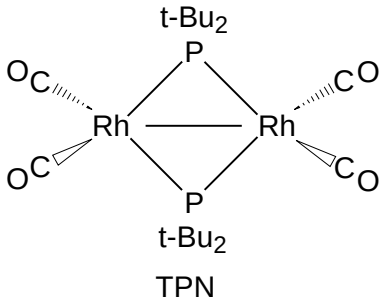

TPN

F8

Cyclic voltammogram of 3.71 mM [Rh(μ-t-Bu$_2$P)(CO)$_2$]$_2$ in tetrahydrofuran/0.5 M [^{n}Bu$_4$N][BF$_4$] at a scan rate of 0.2 V s^{-1} (figure adapted from reference 8).

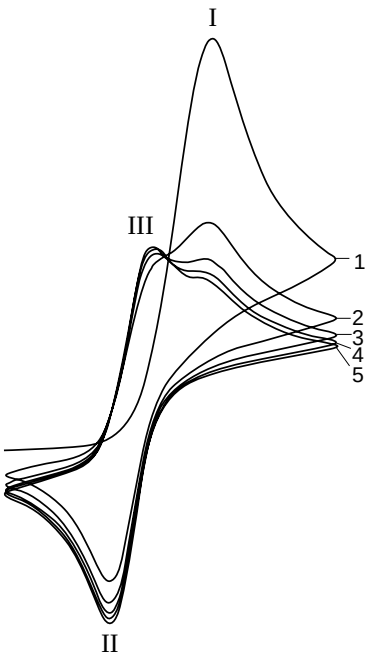

F9

Interconversion of Cp$_2$Rh$_2$(μ-C$_8$H$_8$) and Cp$_2$Rh$_2$(μ-C$_8$H$_8$)$^{2+}$.

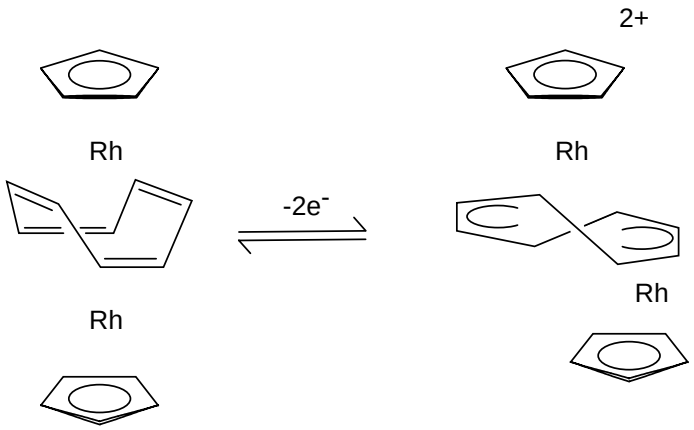

for this change in the ligand coordination mode is the restoration of a (formal) eighteen electron count at the ruthenium center.

Changes in the molecular structure can also occur subsequent to the electron transfer reactions. The cyclic voltammogram for [Rh(μ-t-Bu$_2$P)(CO)$_2$]$_2$ (***F7***) at a scan rate of 0.2 V s^{-1} is shown in ***F8*** (8). This voltammogram is characteristic of an ECE process (a two electron transfer reaction with an intervening chemical reaction). The first electron transfer reaction occurs at I, and is followed by a change from a geometry (labeled TP) in which there is Tetrahedral coordination around one Rh center and Planar coordination around the other Rh center to a geometry (labeled TT) in which the coordination around each Rh center is tetrahedral. The driving force for this structural change is again the attainment of a structure that can more easily accommodate the additional negative charge. Since the TT monoanion can be considered to be electron-deficient, it is more easily reduced than the TP neutral molecule, and hence is reduced immediately upon formation at the electrode surface. Therefore, the peak at I represents a net two-electron reduction. On the reverse scan, the TT dianion is reoxidized to the TT anion at II. Two reductions are observed on the forward scan of the next cycle; the first (III) is due to the reduction of the TT anion (i.e., the II/III couple is due to the TT anion/dianion redox pair), and the second is due to the two-electron reduction of the neutral TP molecule.

Examples of an EEC process have also been reported. The cyclic voltammogram of Cp$_2$Rh$_2$(μ-C$_8$H$_8$) (***F9***) at various temperatures is shown in ***F10*** (9). At room temperature, there is a two-electron oxidation on the forward scan that becomes resolved into two one-electron oxidations as the temperature is reduced. The appearance of a second oxidation peak on the forward scan suggests an EEC process, where the chemical reaction is a change in the coordination mode of the bridging octatetraene ring from η^4,η^4 to η^5,η^5 (***F9***) (this maintains a formal eighteen electron count at each of the metal centers). One effect of the chemical reaction following the second oxidation is to shift the potential required for this oxidation to less positive values. If the rate of the chemical reaction is fast enough, and the separation of the two redox potentials is small enough, then the shift in the potential required for the second oxidation may be sufficiently large that the second oxidation can occur at the potential of the first oxidation, giving rise to a net two-electron process. Lowering the temperature decreases the rate of the chemical reaction. More positive potentials are now required for the second oxidation, and hence the two-electron process becomes resolved into two one-electron processes.

The above examples of two-electron transfers involved transition metal compounds. Two-electron transfers are also very common for organic compounds in aqueous solutions. A simple example of a two-electron transfer is the reduction of 1,4-benzoquinone, and the CVs for this molecule at pH 0 and pH 6 are shown in ***F11A*** and ***F11B***, respectively. It is apparent that both the electron transfer kinetics and the redox potential for this reduction are pH dependent. This can be attributed to the involvement of protons in the electron transfer reactions; the two-electron reduction requires the addition of two protons, and the two-electron oxidation requires the removal of two protons. Therefore, lowering the pH (increasing the proton concentration) facilitates the reduction, but hinders the oxidation, and hence the peaks in the CV are shifted to more positive potentials.

F10

Cyclic voltammograms of $Cp_2Rh_2(\mu\text{-}C_8H_8)$ in methylene chloride at a scan rate of 0.2 V s^{-1} at various temperatures (figure adapted from reference 9).

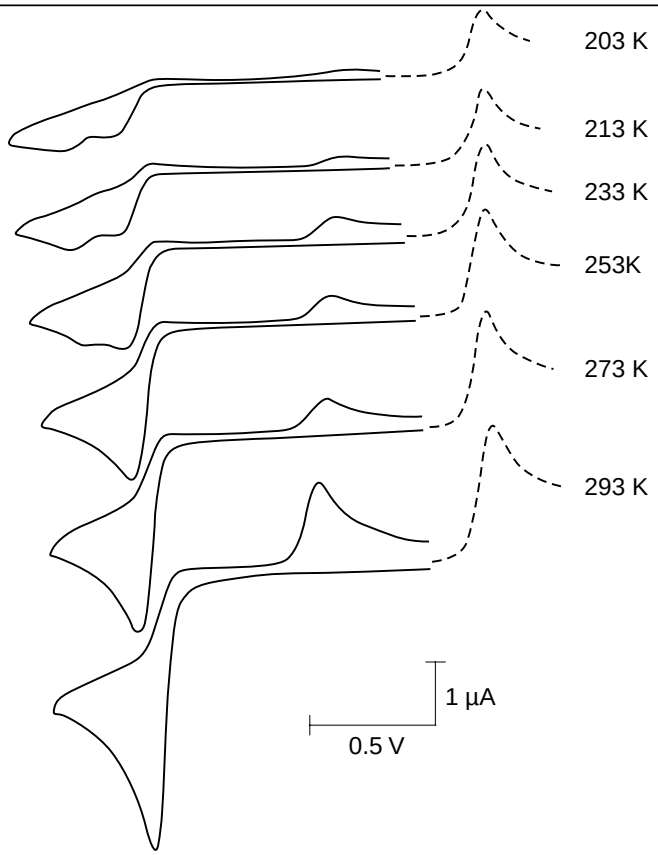

F11

Cyclic voltammograms for 2 mM 1,4-benzoquinone at a scan rate of 0.1 V s^{-1} at (a) pH 0 and (b) pH 6.

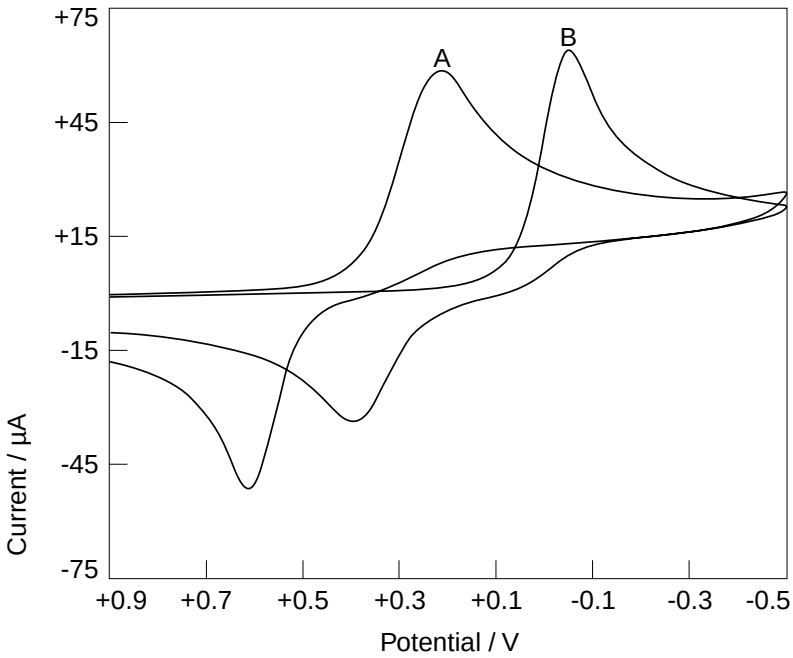

F12

Square scheme for the two-proton two-electron reduction of 1,4-benzoquinone.

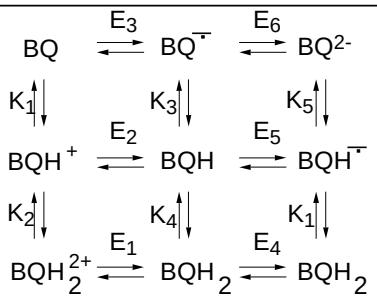

Two-electron two-proton processes are complicated by the existence of three protonation states for each of the two oxidation states. Hence, there are nine species to be considered, with six one-electron transfer processes, and six proton transfer reactions (***F12***). The relative importance of each reaction varies with pH. The simplest mechanisms are the limiting cases, which are proton-electron-proton-electron at low pH, and electron-proton-electron-proton at high pH. However, at intermediate pH, the mechanisms are more complicated.

Digital simulation of two-electron, two-proton transfer processes using the nine species square scheme is complicated, although such studies have been published (10, 11). However, it has been shown (10) that, if the protonation reactions are at equilibrium (i.e., fast relative to the electron transfer reactions) and if $\alpha = 0.5$ for all the electron transfer reactions, then a two-electron, two-proton process mechanism can be represented as two sequential one-electron-transfer processes. The apparent rate constants for each of these one-electron processes are related to the rate constants of the electron transfer processes and the equilibrium constants of the proton transfer reactions of the nine species scheme, and the apparent redox potentials are determined by the redox potentials and proton transfer equilibrium constants.

A digital simulation of the two-electron, two-proton reaction using the "two reaction" model is shown in ***F13*** for the CV of benzoquinone at pH 6. A good fit between the simulated and (background subtracted) experimental data was obtained (the redox potentials, the electron transfer rate constants and the [linked] diffusion coefficients were optimized).

These examples illustrate a variety of ways in which a net "two-electron" process can arise from two one-electron processes. In all cases, it is necessary to consider the overall reaction in terms of the one-

F13

Experimental (line) and simulated (circles) cyclic voltammograms of 2 mM 1,4-benzoquinone at a scan rate of 0.1 V s^{-1} at pH 6.

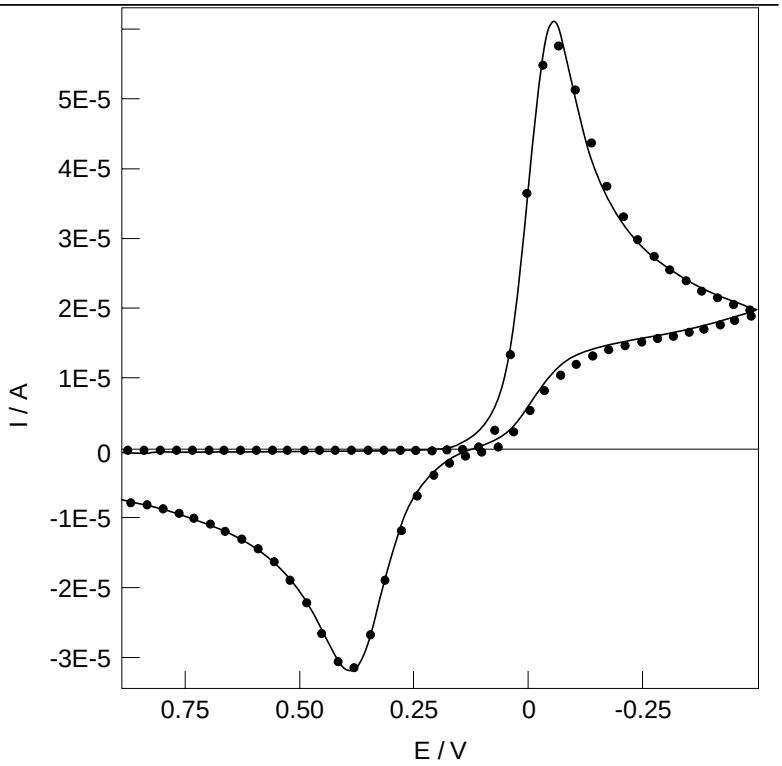

electron reactions and any coupled chemical reactions in order to characterize the process completely.

References

1. R.L. Myers and I. Shain, Anal. Chem. 41 (1969) 980-989.
2. It should be noted that peak separations are temperature dependent. The data quoted in the article are for T = 298 K.
3. J.B. Flanagan, S. Margel, A.J. Bard and F.C. Anson, J. Am. Chem. Soc. 100 (1978) 4248-4253.
4. M.B. Robin and P. Day, Adv. Inorg. Chem. Radiochem. 10 (1967) 247-360.
5. R.H. Cayton, M.H. Chisholm, J.C. Huffman and E.B. Lobkovsky, J. Am. Chem. Soc. 113 (1991) 8709-8724.
6. B. Tulythan and W.E. Geiger, J. Am. Chem. Soc. 107 (1985) 5960-5967.
7. D.T. Pierce and W.E. Geiger, J. Am. Chem. Soc. 114 (1992) 6063-6073.
8. J.G. Gaudiello, T.C. Wright, R.A. Jones and A.J. Bard, J. Am. Chem. Soc. 107 (1985) 888-897.
9. J. Edwin and W.E. Geiger, 112 (1990) 7104-7112.
10. E. Laviron, J. Electroanal. Chem. 164 (1984) 213.
11. M.R. Deakin and R.M. Wightman, J. Electroanal. Chem. 206 (1986) 167.